5.2 Tuning the structure of nanowires by electrodeposition

Tuning the structure of nanowires is important as means of precisely controlling their properties. In the case of template electrodeposition, the dimensions of the nanostructure are predetermined by the template. Therefore, changing the internal structure of the nanowire by the deposition process can be identified as key issue, which must be addressed to further control and tune the properties of nanowires of a given material. In particular, the electrodeposition parameters have a strong influence on the preferred growth orientation and crystal structure.[17] The template-directed electrochemical method has been widely used to produce a large variety of metals, semiconductors, and composite materials. Hence, the influence of deposition parameters on the nanowire structure has been investigated thoroughly, and much research work concerning the growth mechanisms inside high-aspect ratio templates is reported.[34,54,55,154–156] It was demonstrated that the structures of nanowires consisting of various metals can be tuned from typical polycrystalline to single-crystalline.[66,157] However, single-crystal growth via electrodeposition is very difficult for high melting point metals such as Rh and Pt.[14] Since these metals are relatively insensitive to the electrodeposition parameters, additional methods for tuning their structure are desirable. Manipulating their morphology is important for providing control over properties required for applications in the field of catalysts, sensors, and electronic devices.
In this section, methods to produce multilayered and single-element segmented nanowires are demonstrated. The effects responsible for morphological changes also used to manipulate microstructures. The presented results are partially published.[2]

5.2.1 Multilayered nanowires

As frequently demonstrated, it is easily possible to produce multilayered nanowires inside nanochannels of a template material. Here, a method reported by Choi et al. for AAO is adopted to produce Co/Pt nanowires.[36]

Deposition of the multilayered Co/Pt nanowires was carried out from a single electrolyte containing 0.3 mol/L $CoSO_4$, 0.3 mol/L K_2PtCl_6, and 0.485 mol/L H_3BO_3 using a three-electrode setup. Pt segments formed at $U_1 = -0.4$ V, while Co-rich segments were deposited at $U_2 = -1.0$ V with respect to the Ag/AgCl reference electrode. The nanowire growth process could also be carried out with a two-electrode cell.

Figure 5.9 illustrates Co/Pt nanowires that were imaged by scanning transmission electron microscopy (STEM). The readily distinguishable segments consist of different compositions. The more dense Pt structures appear darker than the Co-rich segments. Because of codeposition of the less noble metal, small amounts of Pt are always present in the Co-rich segments.

The transfer of existing methods seems to be uncomplicated and should readily allow to produce multilayered nanowires consisting of other materials.

5.2.2 Segmented single-element nanowires

Here, the synthesis of segmented all-Pt nanowires is presented. The combination of a suitably chosen electrolyte/template system with pulse-reverse electrodeposition allows the formation of well-defined segments linked to nanowires. Manipulation of the morphology is obtained by controlling the electrokinetic effects on the local electrolyte distribution inside the nanochannels during the nanowire growth process, allowing a deviation from the continuously cylindrical geometry given by the nanoporous template. The length of the segments can be adjusted as a function of the cathodic pulse duration. Applying constant pulses leads to segments with homogeneous shape and dimensions along most of the total wire length.

X-ray diffraction demonstrates that the preferred crystallite orientation of the polycrystalline wires varies with the average segment length. The results are explained considering transitions in texture formation with increasing thickness of the electrodeposit. A mechanism of segment formation is proposed

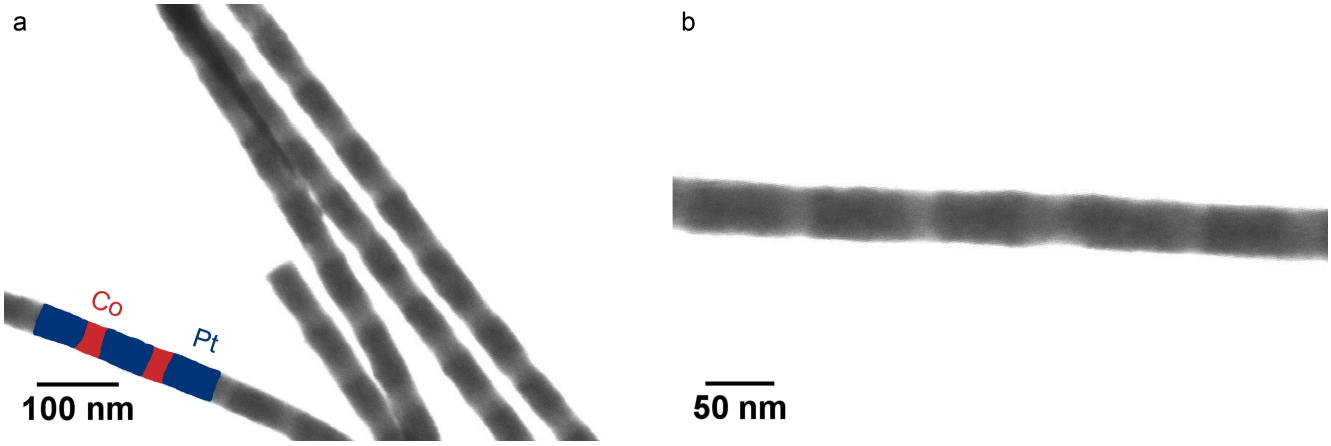

Figure 5.9: STEM images of multilayered CoPt nanowires produced by pulsed electrodeposition from a single electrolyte containing Co and Pt species. (a) Several nanowires show segments of different compositions. Pt segments (blue) and Co rich segments (red) can be identified due to differences in density and atomic number. (b) A single multilayered CoPt nanowire at higher magnification.

based on structural characterizations. Nanowires with controlled segmented morphology are of great technological importance, because of the possibility to precisely control their substructure as a means of tuning their electrical, thermal, and optical properties.

The concept, shown for electrodeposited platinum and track-etched polycarbonate membranes, can be applied to other selected materials as well as templates and constitutes a general method to controlled nanostructuring and synthesis of shape-controlled nanostructures.

Fabrication

Figure 5.10a shows a representative example of a pulse reversed deposition for three consecutive pulses with cathodic pulse duration $t_c = 5$ s and anodic pulse duration $t_a = 1$ s, applied for the growth of modulated Pt nanowires. In addition, the current vs. time response is displayed. It is noticeable that coalescence features following the initial nucleation can be identified.

The curve in Figure 5.10b represents the charge Q_p employed during each pulse as a function of the respective pulse number N, and it shows the same three characteristic zones (1-3) as the current-time curves, recorded for metallic nanowires grown under direct current (dc) deposition conditions.[54,154] After a charge decrease due to the growing linear diffusion layer in zone 1, an almost constant regime is reached in zone 2, while the nanochannels are filled with Pt. Zone 3 represents the rapid increase of charge, as caps are formed on top of the membrane surface enlarging the electrode area. Q_p was calculated by integrating the correspondent current vs. time response, shown in Figure 5.10a. The Faraday law relates the charge needed for each segment growth with the segment's geometrical characteristics. Using

$$Q_p = zF\rho L_s \pi r^2 w/M \tag{5.1}$$

with z denoting the ion charge state, F the Faraday constant, ρ the density of platinum, r the channel/wire radius, w the total number of nanowires, M the molar mass, and L_S the average length of segments, L_S was calculated for each pulse number N corresponding to the segment number. The results demonstrate that the length of the segments can be controlled by the duration of the cathodic pulse, and that the efficiency of the deposition reaction is about 100%.

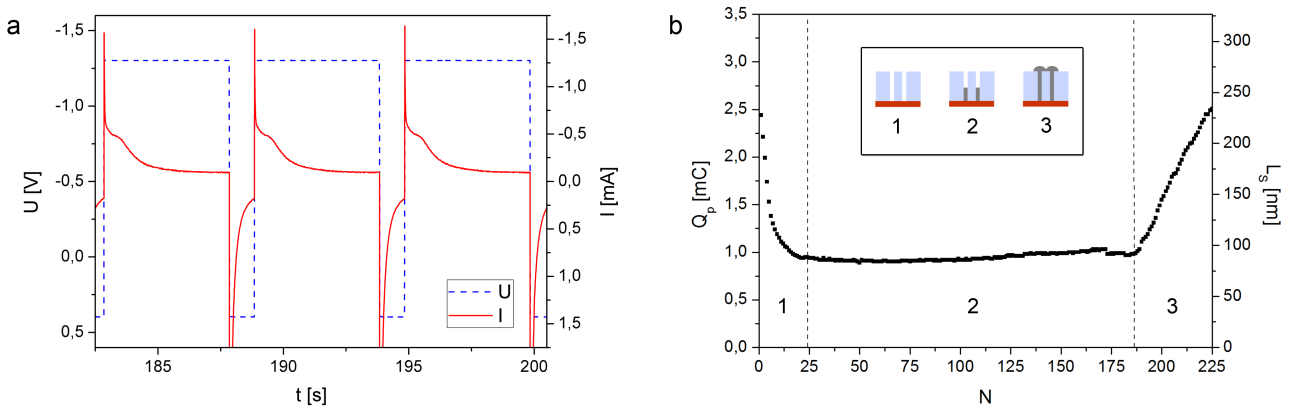

Figure 5.10: Graphs illustrating the pulse-reverse electrodeposition method for the production of segmented nanowires: (a) Applied potential *U* and the resulting current *I* as function of time for three consecutive pulses. (b) Development of the deposited charge of cathodic pulses Q_p and the average segment length L_S with the pulse number *N*. The inset indicates the main events of the three regimes (1-3).

Structural characterization

Figure 5.11 presents FESEM images of Pt nanowires exhibiting their characteristic segmented morphology obtained by PR electrodeposition. Figure 5.11a depicts several nanowires consisting of segments that maintain their homogeneous dimensions (diameter 45 nm, length 50 nm) almost along the entire nanowire. Typically, the nanowires exhibit the same morphologic characteristics over lengths > 20 µm. In addition, high-magnification images (Figure 5.11b,c) reveal both sharp interfaces and pronounced diameter constrictions over the full wire length.

Figure 5.12a and b display nanowires produced by PR deposition using pulse durations t_c = 5 and 20 s, respectively, resulting in current-time transients shown in the insets. The images displaying the sections of the nanowires with lengths 55 and 200 nm, respectively, prove that the segment length can be well controlled as a function of the cathodic pulse duration. By modulating the potential, sequence controlled nanowires can also be produced for potential applications as information storage or barcoded nanowires. The segment length is very uniform along the wire axis. A slight and continuous length increase along the axis proceeds due to the rise in diffusion limited current with growing amount of Pt deposited in the template. With other words, electrodeposition in the membrane nanochannels can be described as occurring on a recessed nanoelectrode array. During nanowire growth, the cathode surface translates towards the upper membrane surface, and thus the effective length of the recessed nanoelectrode decreases continuously. For pulses of the same duration, the electrodeposited segment length will be proportional to the diffusion current. Electrochemical growth of segmented nanowires constitutes therefore a powerful method to investigate transport processes in nanochannels.

Representative TEM images of several segmented nanowires are depicted in Figure 5.13. The selected area electron diffraction (SAED) pattern shown in the inset indicates the polycrystalline structure of the corresponding nanowires. Interestingly, the micrographs reveal that the segments are linked to each other only by a short connection with reduced diameter in the center, rotationally symmetric to the wire axis (Figure 5.13a). The nanowires thus do not fully adopt the morphology of the nanochannels, in contrast to the common behavior when applying dc voltage. Void space observed between the segments is essential to create clear separations. It is evident that these wires exist in a thermodynamic nonequilibrium state, and that the deviation from the cylindrical geometry predetermined by the template is a

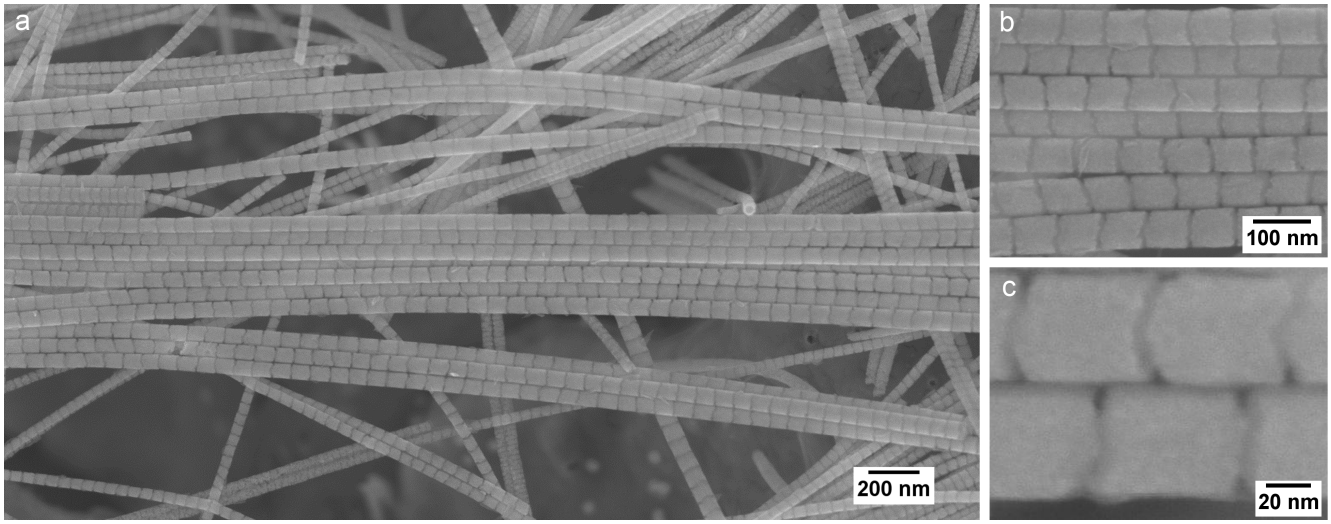

Figure 5.11: FESEM images of segmented Pt deposited under PR with t_c = 5 s at different magnifications (diameter 45 nm).

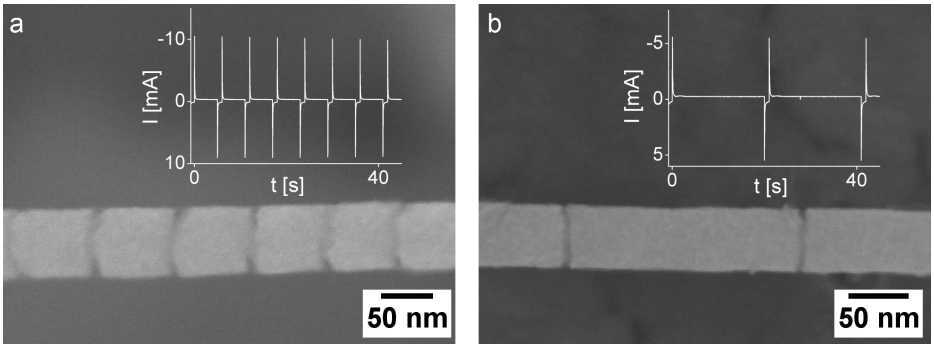

Figure 5.12: FESEM images of segmented Pt nanowires produced with different cathodic pulse durations (t_c = 5 and 20 s, respectively, diameter 50 nm). The insets show corresponding current-time curves recorded during PR electrodeposition.

consequence of a growth process predominantly controlled by kinetics.

To study the influence of the cathodic pulse characteristics on the resulting nanowire morphology, Pt was electrodeposited in different membranes with identical characteristics. Cathodic pulses, all with $U_c = -1.3$ V but different duration t_c = 5, 2.5, and 1 s, were applied while keeping the anodic pulse voltage and duration constant at $U_c = +0.4$ V and t_a = 1 s. TEM images in Figures 5.13b-d demonstrate (as previous images in Figure 5.12) that the segment length decreases with shorter pulse duration t_c, until individual segments can hardly be recognized (Figure 5.13d). However, a complete disappearance of the segmented morphology could also be observed when the cathodic pulse duration t_c was much shorter than 1 s.

The growth mechanism of segmented nanowires is assumed to be based on a slow ion diffusion in the channels, together with a kinetically controlled reduction at the electrode during the cathodic pulse. During the anodic pulse, the ions have additional time to diffuse to the electrode, thus decreasing the concentration gradient in the nanochannel. Consequently, the electrolyte concentration is higher on the electrode surface at the beginning of a deposition pulse and decreases during the cathodic pulse. For very short cathodic pulses, the average ion concentration in the vicinity of the electrode remains high. Appropriate differences in the local electrolyte distribution, essential for segment formation, cannot be

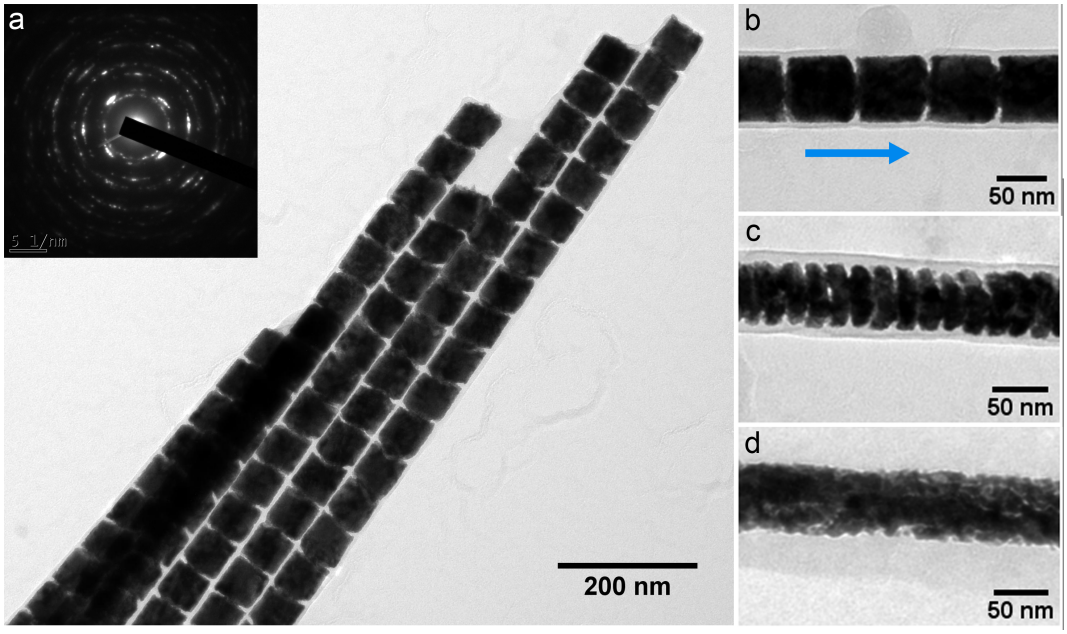

Figure 5.13: TEM images of Pt nanowires produced by PR electrodeposition with different cathodic pulse durations t_c at U_c = -1.3 V: (a-b) segmented nanowires (t_c = 5 s), (c) segmented nanowire (t_c = 2.5 s), (d) continuous nanowire (t_c = 1 s). The anodic pulse was timed to t_a = 1 s at U_a = +0.4 V for all experiments. The inset represents the corresponding SAED pattern.

established. In addition, as the average current density is decreased for short cathodic pulses, the growth process becomes less controlled by kinetics. Hence, the wires appear continuously cylindrical without clear signs of segmentation, but rather displaying irregular grain boundaries, indicating a typical 3-D nucleation-coalescence mechanism (Figure 5.13d).

Texture development

The crystal structure of nanowire arrays, produced by dc and PR deposition with different cathodic pulse durations, was investigated systematically by XRD, while keeping the wires embedded in the template. These arrays were deposited in templates fabricated in exactly the same manner, leading to arrangements of similar wire diameter, length, and areal density. The related X-ray diffractograms shown in Figure 5.14a demonstrate that the crystallographic orientation is sensitive to variation of the deposition parameters. A correlation of segment length with texture is observed. In particular, significant changes are found with regard to ⟨200⟩ reflections.

In the case of dc deposition and PR deposition using long cathodic pulses of 20 s, the wires are continuously cylindrical or composed of long segments, and appear rather polycrystalline without preferential orientation. With decreasing pulse duration t_c (from 20 to 5 s) and segment length (from 139 to 50 nm), the intensity of the ⟨200⟩ reflection becomes stronger as a distinct preferred orientation in the ⟨100⟩ direction is developed. Further decrease in cathodic pulse duration leads again to a polycrystalline structure with random orientation.

This observation is supported by texture coefficients TC_{hkl} calculated by equation 4.1 (page 36) for the different *hkl* reflections considering the first four reflections (111, 200, 220, and 311; Table 5.4). The theoretical maximum value of TC is 4, representing nanowires with all crystallites oriented in the same direction along the wire axis. The texture coefficient TC_{100} of the Pt wires is plotted versus the

Table 5.4: Texture coefficients of nanowire arrays with different average segment length L_S.

L_S [nm]	TC_{111}	TC_{100}	TC_{110}	TC_{311}
13.2	1.00	1.10	1.00	0.91
29.5	0.67	2.09	0.39	0.85
50.3	0.50	2.35	0.41	0.73
74.1	0.56	1.94	0.55	0.95
138.8	1.03	0.99	0.88	1.09

average segment length in Figure 5.14b. It reaches its highest value of 2.35 for a cathodic pulse duration of 5 s. The average segment length was calculated using Faraday's law and experimentally determined by FESEM, as explained above.

The development of a preferred growth orientation is assumed to be caused mainly by nucleation and growth of crystallites during the cathodic pulse and not during postdeposition processing. Because different crystal faces show different rates of growth, crystallites with different orientations compete in growth rate. The generation of a preferred orientation of the crystallites can be either an effect of preferential nucleation, or can originate from the competitive growth process following the coalescence stage.[158,159] Assuming the second case, texture formation is a process that develops with deposition time and thickness of the deposit. Transitions in phase formation have been observed, and it was shown that after a critical thickness is reached, phase formation changes from a thermodynamically to a kinetically controlled process.[160,161] Since preferred orientation, created during the initial step of electrodeposition, often deviates from the orientation of the crystallites formed during following growth, the deposit texture and its degree of perfection will finally be controlled by the thickness of the electrodeposit.[162]
In the case of segmented nanowires, the segment length is identical with the deposition thickness. It is assumed that nearly all segments of a sample are almost identical, regarding the development of texture along their axis, because the electrodeposition conditions before each deposition pulse and mass transport during growth are very similar. By investigating samples with segments of different lengths, information about the development of preferred orientation is obtained. The experimental results reported in Figure 5.14 show that segments differing in length have different textures. Therefore, a transition in phase formation must occur after a critical thickness is reached. The shortest observed deposits, measuring an average thickness of 13.2 nm, exhibit no clearly preferred orientation, with all considered TC_{hkl} values close to 1. By increasing the average segment length to 29.5 nm, a preferred orientation in the ⟨100⟩ direction appears.

It may be suggested that in the initial stage of electrocrystallization the orientation of the Pt nuclei is random, leading to a newly coalesced deposit with random orientation. The texture of thicker deposits is a result of competitive growth mechanisms of crystallites, taking place in a stage of growth subsequent to the coalescence stage. Grains of low surface energy grow faster than those of high surface energy. After formation of the first layers, the {100} surface, representing a low-energy surface, is favored. Consequently, a ⟨100⟩ texture is developed as the fraction of crystallites oriented in this direction prevails. The degree of perfection of the ⟨100⟩ texture increases with the average segment length, until it reaches a maximum for segments with an average length of 50.3 nm. As the cathodic pulse duration is further increased to grow longer segments, the period of time of each pulse, in which the reduction reaction is limited by the diffusion-driven transport, is expanded. The gain of the diffusion limited regime shifts the process towards a mechanism being mainly controlled by kinetics, allowing energetically higher surfaces such as the {311} and {220} surface to grow increasingly, and hence the ⟨100⟩ texture vanishes. The structure becomes rather randomly oriented, again for segments with an average length of 138.8 nm and cylindrical nanowires produced under dc.

The average size of crystallites oriented in the ⟨100⟩ direction was derived from the full width at half maximum (FWHM) of the Pt 200 reflections in the diffractograms presented in Figure 5.14a (according

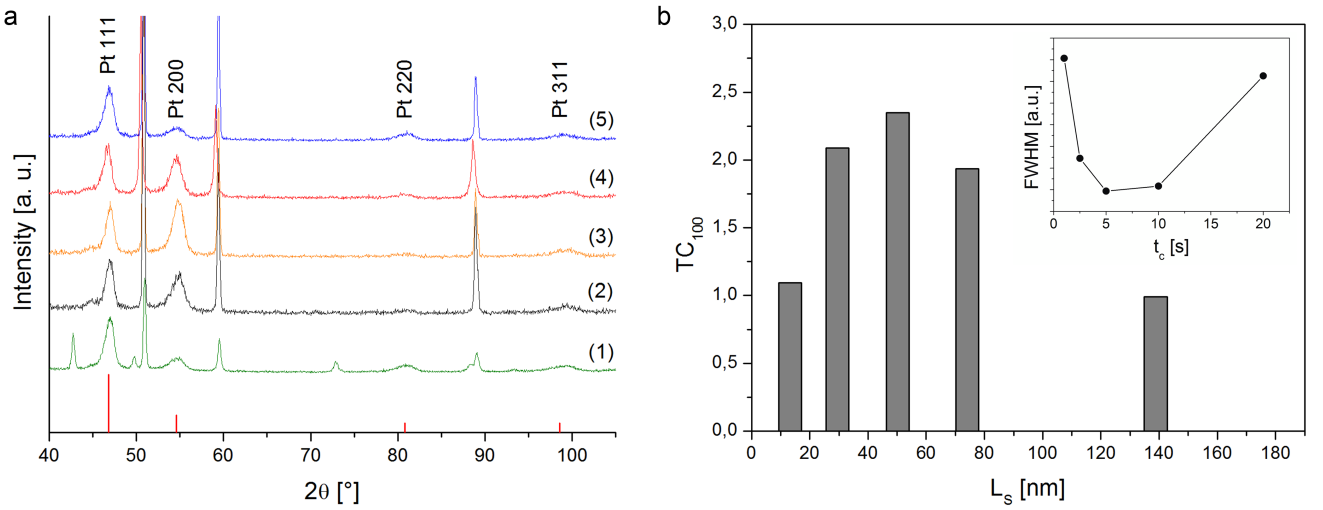

Figure 5.14: (a) X-ray diffractograms of segmented nanowire arrays produced by PR electrodeposition (1-5) using different cathodic pulse durations (1, 2.5, 5, 10, and 20 s). Peaks not labeled originate from Cu and CuO in the cathode layer. Vertical lines represent the intensity distribution of a Pt powder sample. (b) TC_{100} versus segment length. The inset shows the development of the FWHM of the Pt 200 reflexes.

to Scherrer equation). The development as a function of t_c is plotted in the inset of Figure 5.14b. The average size of the crystallites with ⟨100⟩ orientation increases with the segment length. This finding may be a result of the preferred growth of existing crystallites with ⟨100⟩ orientation and hints to a granular texture. Finally, as the segments grow longer, the average size of grains with ⟨100⟩ orientation appears smaller again, since the deposition conditions favor increasingly surfaces other than {100}. Thus, the fraction of smaller crystallites oriented in the ⟨100⟩ direction increases with the average segment length. Estimations using the Scherrer equation result in grains with ⟨100⟩ orientation of an average size of $5 - 7$ nm. These results are in good agreement with observations made by TEM.
It has to be carefully considered that increasing t_c without changing t_a leads to a decrease of the average electrolyte concentration near the growing nanowire. As a consequence, limitations due to mass transport gain influence even at the beginning of a deposition pulse. Phase formation becomes more and more controlled by kinetics, and the transition to the development of a polycrystalline deposit with random orientation should start earlier along the segment.
Moreover, it should be taken into account that structural changes in the nanowire-electrolyte interface induced by anodic pulses may also contribute to the development of texture of electrodeposited nanowires.[163] However, since only the electrode surface is affected, the influenced fraction of volume is relatively small under the applied conditions and may only be important for very short cathodic pulses.

Proposed growth mechanism

Different growth processes have been proposed for nanowires.[34,66] The polycrystalline Pt nanowires produced by dc plating seem to follow a typical 3-D nucleation-coalescence mechanism.[65] Several nuclei are formed at the same time, independently of each other, on the layer growth front and grow to 3-D clusters. As deposition is continued, isolated clusters coalesce, and the free space between clusters is subsequently filled until a complete hole-free film is created.

In contrast to the typical 3-D nucleation-coalescence growth mode, the formation of a continuous deposit is not observed for Pt nanowire deposition in the case of PR plating. The SEM and TEM images indicate that nucleation and growth of 3-D clusters occur only on a circular area at the center of each

nanochannel, when a cathodic pulse is applied at the initial state of segment growth. It is believed that the localized formation of nuclei, and thus also the parabolic shape of the segment front faces (Figure 5.13b-c), is directed by the Pt ion concentration and is a direct consequence of the influence of electrokinetic effects on the local electrolyte distribution in small fluidic nanochannels.

Due to the combination of etched ion-track PC membranes and the strong alkaline Pt electrolyte solution, the nanochannel walls acquire a negative charge, and an electrical double layer (EDL) of significant thickness is established.[164] While the negative charges on the channel walls remain stationary, the mobile charges in the EDL result in a flow towards the cathode, if an electrical field is applied. This flow depends on the thickness of the EDL, which in turn depends among other things on the pH-value and the ion concentration and increases with rising pH and a decrease in the electrolyte concentration. For fluidic nanochannels the flow profile is parabolic in shape and becomes more pronounced for increasing double layer thicknesses.[63] This means that the ion velocity is higher in the center of the nanochannel than near the channel wall.
Although the overall mass transport in the nanochannels closed from one side is driven by diffusion, electrokinetic processes can exert a strong influence. In particular, when the external field is reversed, the interactions are expected to be strong in the vicinity of the growing nanoelectrode where the electrolyte concentration is low. This exactly happens, whenever deposition is stopped or when a new segment is deposited. During the anodic pulse, the positive Pt-ions are rejected from the front face of the segment formed immediately before. By applying a cathodic pulse, the ions follow the reversed field and move towards the nanowire. Because of the transport profile the ions move fastest in the very center of the nanochannel. The redistribution of ions leads to local charge differences.

Figure 5.15a shows a schematic illustration of the proposed concentration-directed nucleation-coalescence growth process. At the center of the growth front, the concentration of the Pt species is higher than near the channel wall and hence is also the nucleation rate. It is assumed that after the stage of coalescence, a stable growth process occurs at which a parabolic shape of the growing front is maintained in the majority of cases resulting in parabolic shaped segments at the top side (Figure 5.15b). The whole mechanism is not understood entirely, and further investigations are underway. Our concept may be applied to other suitably chosen systems, to create segmented nanowires consisting of other materials, and represents a general route to controlled nanostructuring.

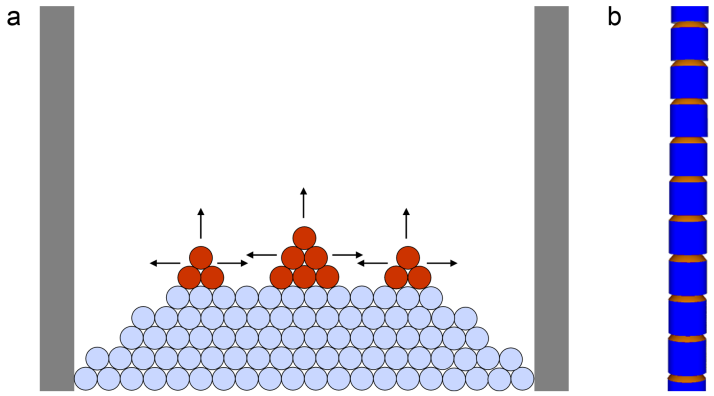

Figure 5.15: (a) Scheme of concentration-directed 3-D nucleation-coalescence growth mechanism. (b) Schematic illustration of a segmented nanowire with parabolic front faces of the segments (shown in red).

5.2.3 Length and sequence controlled Pt nanowires

With one or more different structure elements, barcoded nanowires can be created. The distinguishability of segments forming barcoded nanowires usually relies on differences in the composition between adjacent segments, while the wire is continuously cylindrical along its axis. Only very few reports demonstrate barcoded structures exhibiting segments that have the same composition but vary in diameter or density.[40] These fabrication methods require post-deposition processes to generate distinguishable structure elements. Single-element barcoded nanowires have not been reported so far by a direct electrodeposition approach using cylindrical nanochannels inside a template material.

Here, segmented all-platinum nanowires consisting of segments of two different lengths were fabricated by a sequence of pulses to store binary information; the basic concept described in the previous section was used for synthesis (5.2.2, page 54). Long segments with an average length of 54.8 nm were produced by pulses of 5 s at −1.3 V and shorter segments of 27.3 nm by pulses of 2.5 s at −1.3 V. Between two cathodic pulses, an anodic pulse at +0.4 V was applied for 0.5 s to clearly separate the segments. Figure 5.16 illustrates the fabricated nanowire structures.

Deposition of two distinguishable structure elements allows the implementation of binary information. For the purpose of demonstration, a single-element segmented nanowire was used to store text by a binary character-encoding scheme based on an eight-bit code. The longer segments (blue) stand for "1", while "0" is represented by shorter segments (red). The inset of Figure 5.16 shows parts of these nanowires consisting of two different types of segments. The micrograph clearly illustrates how the two different segments can form a signature.

The use of an eight-bit code, such as an ASCII (American Standard Code for Information Interchange) based code, allows the generation of about 100 striping patterns in a 30 µm long nanowire.

The number of possible striping patterns can be rapidly increased by creating more than two different structure elements forming a sequence along the wire axis. With the number of distinguishable segments in a sequence, the number of distinct codes increases dramatically. In general, the number of distinct codes is given by n^m, where n is the number of different segments and m represents the number of segments in a striping pattern.

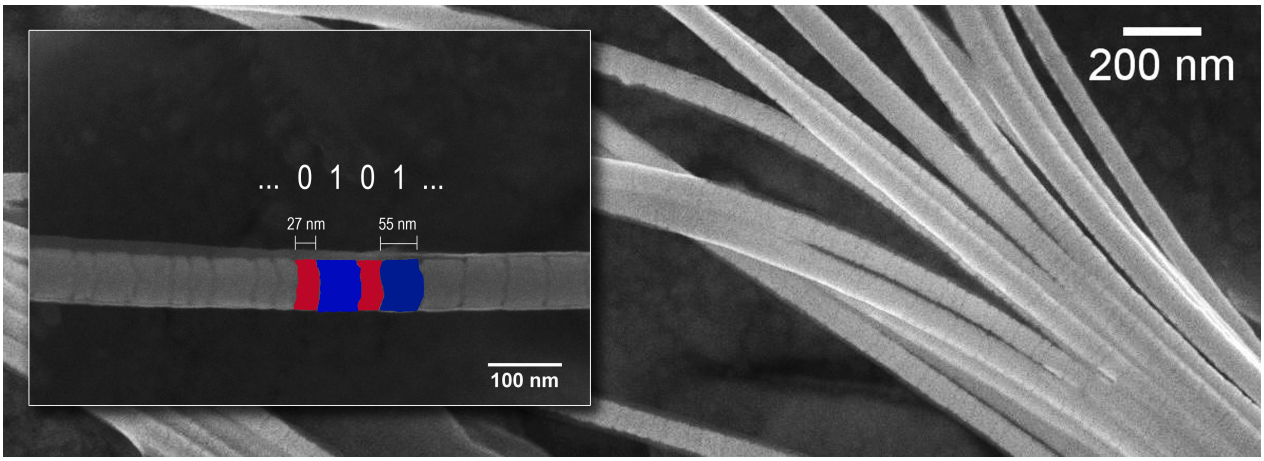

Figure 5.16: SEM images of binary encoded segmented nanowires produced by modulating t_c to create two distinguishable structure elements. The inset shows a part of a nanowire with short (red) and long segments (blue), corresponding to, e.g., "'0"' and "'1"' in a binary code.

5.2.4 Impact of electrokinetic effects on microstructure growth

The impact of electrokinetic effects on growth processes is also visible in larger structures than nanowires. Microwires and caps, forming on top of nanowires, can be structured at surfaces that grow in contact with the polycarbonate foil using PR electrodeposition.

Structured microwires

Figure 5.17 depicts sub-micrometer wires that were produced using PR electrodeposition at 65 °C. The cathodic pulses were applied for 5 s at −1.3 V, while the anodic pulses were timed to 1 s at +0.4 V. The wires appear cylindrical with a smooth surface (Figure 5.17a). At higher magnification, FESEM reveals a regular pattern on the wire surface (Figure 5.17b). Groove-like depressions run perpendicular to the wire axis. Regular spacings between adjacent grooves are apparent with an average distance of 60 nm between two grooves. The dimensions of these recessed nanostructures are uniform with respect to both width and depth exhibiting an average groove width of approximately 5 nm.

As origin of the formation of regularly spaced surface structures on electrodeposited submicro- and microwires the same reasons, which lead to the generation of segmented nanowires, may be accountable. The local electrolyte distribution is influenced by electrokinetic effects arising from the EDL in combination with an applied electrical field. It is assumed that during the anodic pulse, the Pt ions are rejected from the wire surface. Electrocrystallization starts as the cathodic pulse is applied. During this initial stage of phase formation, the ion concentration in the electrolyte volume near the channel wall and the electrode is still depleted. As a consequence, Pt is not deposited in this region and a small deviation from the cylindrical shape is created. After a few nanometers, the growth front transcends the volume of depletion and extends again over the whole channel area.

In contrast to segmented nanowires, the produced structures can affect only a small volume of the wires, because the EDL is very short in comparison to the channel and wire diameter. Moreover, the diameter constrictions are not always perpendicular to the wire axis in the case of microstructures, probably due to fluctuations in electrolyte concentration on a smaller length scale than the electrode surface.

The demonstrated possibility to introduce controlled surface structuring is very interesting for various applications, since surface properties can precisely be influenced.

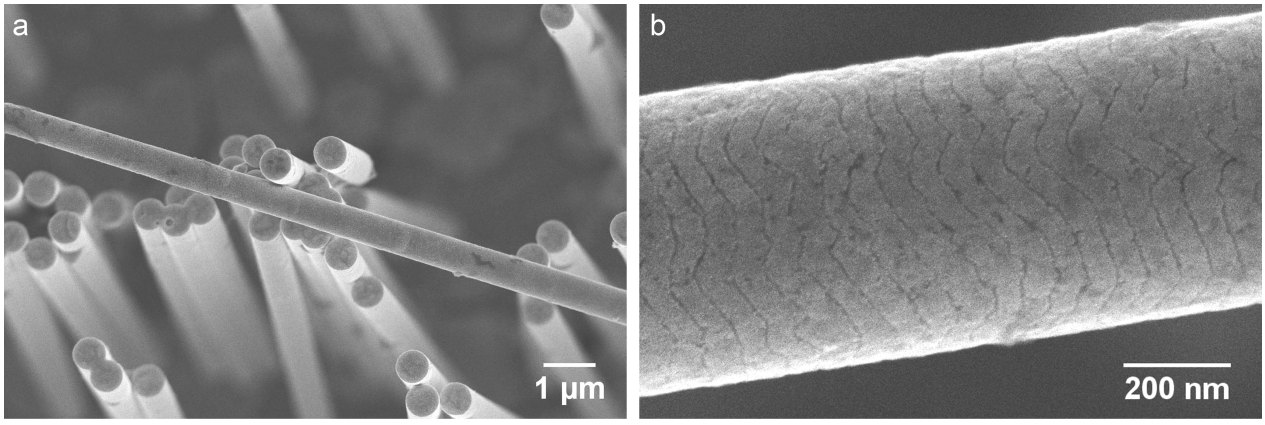

Figure 5.17: SEM images of structured sub-micrometer wires. The wires with an average diameter of 0.6 μm were produced by PR electrodeposition. The surface is structured by regularly spaced grooves that formed due to manipulations of the local electrolyte distribution by electrokinetic effects.

Cap formation during PR deposition

As a growing nanowire reaches the and of a nanochannel, it is no longer confined to the channel geometry and a cap forms on top of the wire. Usually, the cap is hemispherical in shape, since the growth front extends towards the hemispherical diffusion field.

Caps that were grown using PR electrodeposition are comparable to those grown under dc conditions except for the structure of their lower side. Figure 5.18a-c show FESEM images of a representative cap produced by PR deposition. The lower side of the cap appears as disk in the low-magnification image (Figure 5.18a). At higher magnification, the surface structure becomes visible (Figure 5.18b-c). Groove-like structures are arranged on the surface forming concentric circles with regular spacings. Cap growth started at the very center of the lower side of the cap where a bundle of nanowires, which first reached the template surface, is still connected to the cap. The growth direction of these nanowires is indicated by an arrow (Figure 5.18). The formation of the circular structures can again be explained by redistributions of local electrolyte distributions induced by electrokinetic transport processes.

In the case of constant pulse durations, the thickness of an electrodeposit, created during a deposition pulse, is proportional to the diffusion current. Investigations of the distances between adjacent circular structures allow the reconstruction of changes in diffusional mass transport with deposition time (Figure 5.18b). The thicknesses of the circular layers is continuously decreased with the number of deposition pulses; the thickest layers are visible in the center (Figure 5.18c), while the thinnest are located near the edge of the cap.

A newly formed cap on top of the wire establishes a hemispherical diffusion field. As the size of the cap is increased, linear diffusion increasingly contributes to the diffusion process. Although the total current increases with the growing electrode area, the current density is decreased due to the ongoing transition between hemispherical and linear diffusion.

While the growing cap increases its size, nanochannels, which are not completely filled, are covered by the lower side of the cap. In these covered channels, the deposition proceeds in addition to the normal growth direction from top down as indicated by red and blue arrows, respectively (Figure 5.18d). Because the channels are closed from both sides, the ion concentration is depleted after a short time and the nanochannels can not completely be filled with the remaining metal content, resulting in a porous deposit that consists of loosely bound particles. The structure of nanowires growing from the cap inside the nanochannels becomes increasingly porous as deposition is continued until the growth process comes to a rest. In comparison to a cylindrical nanowire, the porous structure is mechanically less stable and could only be imaged by FESEM because of polymer residues stabilizing the structure. Wire fragments that started to grow from the lower side of the cap are depicted in Figure 5.18d.

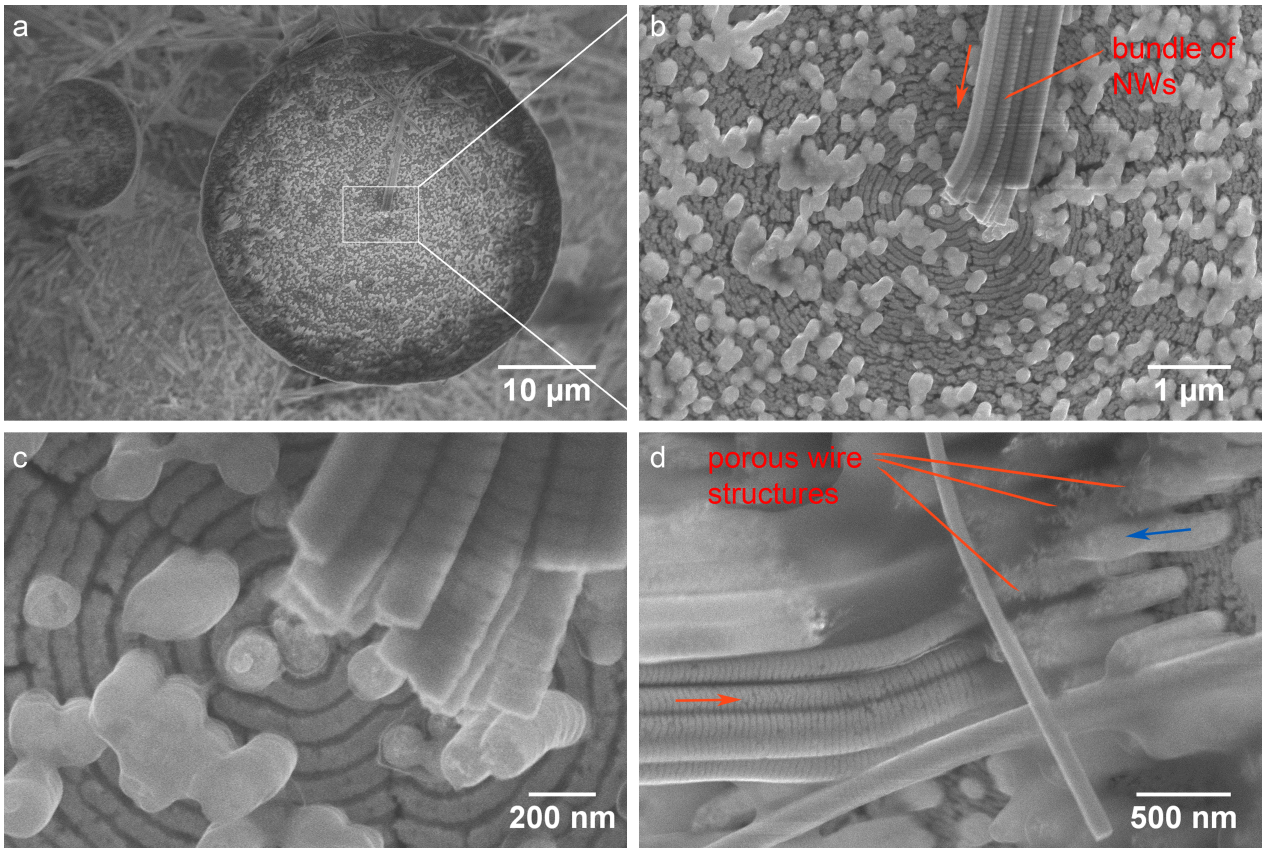

Figure 5.18: FESEM images of structured caps. (a) The lower side of a cap, which was grown on top of a bundle of nanowire using PR deposition, is appears as a disk. (b-c) At higher magnification, a regular structure formed by circular grooves can be identified. Cap growth started at the very center of the lower side of the cap. The growth direction of the nanowires that are still connected to the cap is indicated by an arrow. (d) As the cap grows, nanochannels can be covered by the lower side of the cap. Consequently, growth proceeds in addition to the normal growth direction (red arrow) from top down as indicated by a blue arrow. Wire fragments that started to grow from the lower side of a cap inside closed nanochannels have a porous structure because of the depletion of electrolyte concentration.